Reflection coefficients of fractured rocks: A numerical study

O. S. Krüger, E. H. Saenger, and S. A. Shapiro

email: *krueger@geophysik.fu-berlin.de*

keywords: *reflection coefficient, fractured media, finite difference, modeling*

ABSTRACT

In this work we estimate the effective reflection coefficients of an interface between a cracked and an uncracked material. The study is based on computer simulations using the rotated staggered grid finite difference method. The numerically obtained reflection coefficients are compared to several theoretical predictions from static effective medium formulations. The agreement between our numerical data and the theoretical predictions is best for the differential schemes. This result is supported by previous studies dealing with transmission *experiments.*

INTRODUCTION

Theoretical effective medium descriptions of fractured media are commonly derived from static considerations (see e.g. Mavko et al., 1998, and references therein). Alternatively, numerical estimations of the effective elastic properties of such media have been successful Arns et al. (2002); Saenger and Shapiro (2002); Orlowsky et al. (2003). As the acoustic impedance is altered by the presence of cracks, interfaces between fractured and unfractured materials act as a reflecting boundary for elastic waves. For example, fault zones usually are associated with fractured zones. Recognising their characteristics in seismograms and the knowledge of their reflection coefficients are therefore of great interest in seismic exploration. These reflection coefficients, giving the ratio of the amplitudes of reflected to incident waves, describe a dynamic process. The question we pose in this paper is whether reflection coefficients, which are derived from the static elastic moduli gained from effective media theories, can be used to understand the dynamic process of wave reflection, including effects like the dependence of the reflection coefficients on the angle of incidence (i.e. AVO or AVOZ, see e.g. Castagna and Backus, 1993). As no analytical solutions to the wave equation exist for complex situations like strongly cracked solids, we rely on a numerical finite difference (FD) technique, the rotated staggered grid, to numerically simulate wave propagation and to determine reflection coefficients of the interface between cracked and uncracked areas. The rotated staggered grid as described in Saenger et al. (2000) allows one to simulate wave propagation in highly heterogeneous media without implementing explicit boundary conditions and without averaging elastic moduli. It has been proven to yield stable and realistic results for cracked media Krüger et al. (2002). Our experiments consist of simulations of two dimensional models with a plane wave source at the top of the model illuminating a cracked region at some distance from the source. We present numerical results for the reflection coefficient for normal incidence on cracked areas with different

- crack densities,
- inclination of the cracks,
- dominant frequencies of the source wavelet

and compare them with theoretical predictions. Further parameter variations, which remain to be done, may include the extensions of the cracked region, an inclination of the cracked region and the position of the source.

THEORETICAL PREDICTION OF REFLECTION COEFFICIENTS IN CRACKED MEDIA

Effective medium theories usually predict static elastic moduli. From these moduli, wave propagation velocities, acoustic impedances and hence reflection coefficients can be calculated. Here we focus on three theoretical predictions for parallel cracks, aligned along the x-axis. These are the non-interacting approximation (NIA), the differential scheme (DS) and an extension of the differential scheme (EDS). All theories are discussed in detail in Orlowsky et al. Orlowsky et al. (2003) and references therein. For the NIA, the energy that is needed to insert a single crack into an uncracked medium is simply added to the elastic potential of the medium. The DS recalculates the effective elastic moduli after the insertion of each crack, thus taking the effects of the so far inserted cracks into account. The EDS works like the NIA but multiplies the energy increment for each crack with a function which is derived from expressions for effective moduli corresponding to the DS results for a isotropic crack distribution. Predictions from these theories are given as a function of the crack density ρ_{cd}, which is defined for N cracks of radii a_i distributed over an area A Bristow (1960):

$$\rho_{cd} = 1/A \sum_{i=1}^{N} a_i^2. \tag{1}$$

Young's modulus E_2 along the z-axis and shear modulus G for a crack density ρ_{cd} parallel to the x-axis are then given by:

$$\begin{array}{lcl} E_2(NIA) & = & E \cdot [1 + 2\pi\rho_{cd}]^{-1}, \\ E_2(DS) & = & E \cdot e^{-2\pi\rho_{cd}}, \\ E_2(EDS) & = & E \cdot [1 + 2\pi\rho_{cd} e^{\pi\rho_{cd}}]^{-1}, \\ G(NIA) & = & G \cdot [1 + \pi\rho_{cd}(1-\nu)]^{-1}, \\ G(DS) & = & G \cdot e^{-\pi(1-\nu)\rho_{cd}}, \\ G(EDS) & = & G \cdot [1 + \pi\rho_{cd}(1-\nu) e^{\pi\rho_{cd}}]^{-1}, \end{array} \tag{2}$$

where E denotes the Young's modulus and ν the Poisson's ratio of the background matrix. Note that E_1 (along the x-axis) equals E, which means that it is not affected by the cracks. Using these effective moduli, the stiffness matrix for cracks parallel to the x-axis can be calculated according to

$$\begin{bmatrix} < c_{11} > & < c_{12} > & 0 \\ < c_{12} > & < c_{22} > & 0 \\ 0 & 0 & < c_{44} > \end{bmatrix} = \begin{bmatrix} \frac{1-\nu^2}{E_1} & -\frac{\nu(1+\nu)}{E} & 0 \\ -\frac{\nu(1+\nu)}{E} & \frac{1-\nu^2}{<E_2>} & 0 \\ 0 & 0 & \frac{1}{<G>} \end{bmatrix}^{-1} . \tag{3}$$

The corresponding effective velocities follow from:

$$v_{P,eff} = \sqrt{c_{22}/\rho_{g,eff}}, \quad v_{S,eff} = \sqrt{c_{44}/\rho_{g,eff}}. \tag{4}$$

The normal-incidence reflection coefficient R_{PP} of an interface between two materials with velocities $v_{P,1}$ and $v_{P,eff}$, resp., and densities ρ_1 and ρ_{eff}, resp., is given by:

$$R_{PP} = \frac{v_{P,eff}\rho_{eff} - v_{P,1}\rho_1}{v_{P,1}\rho_{g,1} + v_{P,eff}\rho_{eff}}. \tag{5}$$

MODELING PROCEDURE

The two dimensional models consist of a homogeneous medium. Into the lower part of that medium dry cracks are placed, varying in number and inclination for different simulations. Different types of wavelets (Gaussian type and Ricker I) and dominant frequencies (f_{dom}) are used for the plane wave, which propagates from the top of the model downwards (see Fig. 1Tab. 2). The dimension of the models is 1501

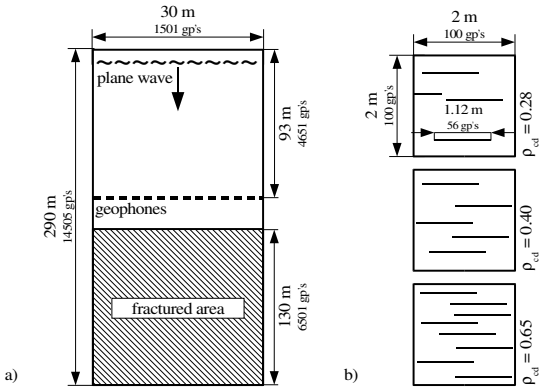

Figure 1: a) Typical numerical setup (not to scale). Receivers are places at a depth of about $93m$ (dashed line). The plane wave propagates from the top of the model downwards (arrow) towards the cracked area. b) Three exemplifications for a given area (here: $A = 4m^2$), crack length ($2a = 1.12m$) and crack density (ρ_{cd}) of a fractured region. The number of cracks increases with the crack density, hence the cracks are closer-packed.

	homogeneous medium (matrix)	dry crack
$v_p\ (m/s)$	6000.0	0.0
$v_s\ (m/s)$	3454.0	0.0
$\rho\ (kg/m^3)$	2500.0	$1 \cdot 10^{-6}$

Table 1: Compressional-wave velocity (v_p), shear-wave velocity (v_s) and density (ρ_g) of the homogeneous medium and the cracks are listed here.

grid points in the x-direction and 14505 grid points in the z-direction with a grid point spacing of $0.02m$ in both directions. The fractured region starts at a depth of 8005 grid points. The elastic parameters of the medium and cracks are specified in Table 1. The crack length is $2a = 1.12m$ in all models. Two types of crack distributions have been used, parallel aligned cracks and cracks with a random inclination $\alpha \in [-15^o,\ 15^o]$. Receivers are placed at a depth of 4651 grid points. The reflection coefficient is then calculated from the ratio between the mean amplitude of the reflected wave field and the amplitude of the source wavelet.

NUMERICAL RESULTS

The reflection coefficients according to the predictions from the static effective medium formulations and our numerical determined reflection coefficients are plotted in Fig. 2. For the parallel cracks and the inclined cracks one observes an excellent agreement between our data and the predictions from the extended differential scheme (EDS), while the difference to the NIA prediction is significant. Since the theoretical predictions of the reflection coefficients are based on *static* elastic medium theories the dynamic simulations have to be conducted in the long wavelength limit, meaning that the wave length has to be very large compared to the crack length. To accomplish this we have chosen a Gaussian like wave form, which has a high low-frequency content. In addition we used have a Ricker I wavelet (first derivative of a Gaussian) to represent a more realistic wave. Using Ricker I wavelet instead of Gaussians and going to high frequencies, resulting in shorter wave length and smaller wavelength to crack length ratios, we see the increased mismatch of the theoretical predictions and the numerical results increase. This is to be expected as we are leaving the long wave length limit. The match between our data and the results from the differential scheme is also very satisfying. This is in agreement with previous results from transmission experiments presented by Orlowsky et al. Orlowsky et al. (2003).

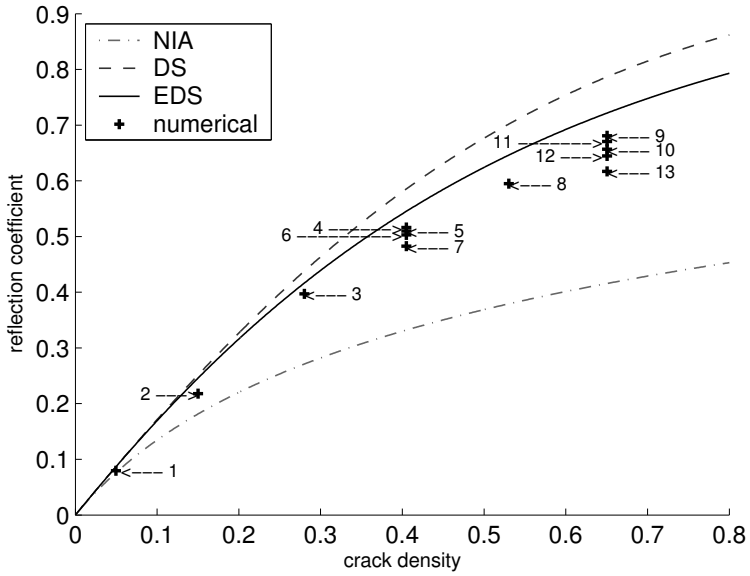

Figure 2: Reflection coefficients for models with parallel cracks. The reflection coefficient according to different theories are plotted as lines. Our numerical results are represented by plus signs. The numbers at each numerical result corresponds to the modell number (see Tab. 2).

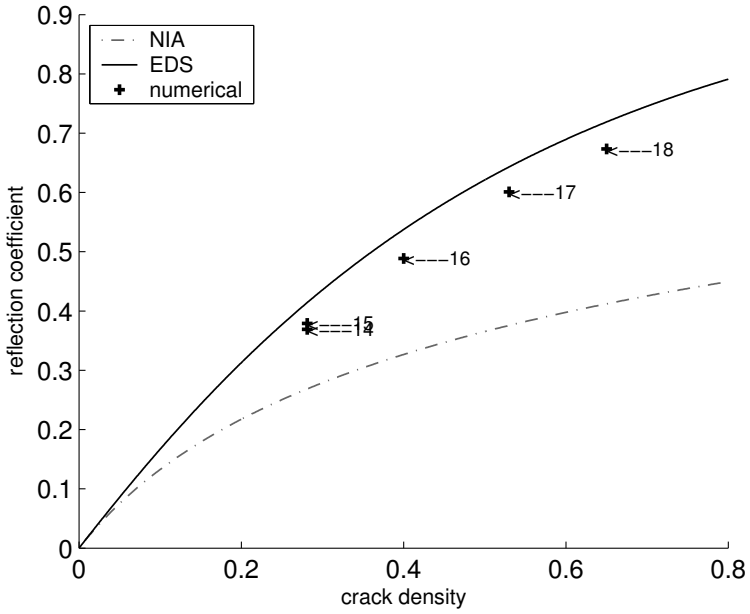

Figure 3: Reflection coefficients for models with $\pm 15^o$ inclined cracks. This inclination influences the theoretical predictions and requires a slightly modified crack density tensor. For details refer to Orlowsky et al. (2004). The reflection coefficient according to different theories are plotted as lines. Our numerical results are represented by plus signs. The numbers at each numerical result corresponds to the modell number. (see Tab. 2)

model number	ρ_{cd}	source signal and f_{dom} (Hz)	inclination of the cracks (^{o})	relation: wave length/ crack length
1	0.05	Gaussian, 300	0.0	≥ 17
2	0.15	Gaussian, 300	0.0	≥ 17
3	0.28	Gaussian, 150	0.0	≥ 36
4	0.40	Gaussian, 150	0.0	≥ 36
5	0.40	Gaussian, 300	0.0	≥ 17
6	0.40	Ricker I, 300	0.0	17
7	0.40	Ricker I, 600	0.0	9
8	0.53	Gaussian, 150	0.0	≥ 36
9	0.65	Gaussian, 150	0.0	≥ 36
10	0.65	Gaussian, 300	0.0	≥ 17
11	0.65	Ricker I, 150	0.0	36
12	0.65	Ricker I, 300	0.0	17
13	0.65	Ricker I, 600	0.0	9
14	0.28	Ricker I, 150	± 15	36
15	0.28	Ricker I, 600	± 15	9
16	0.40	Ricker I, 150	± 15	36
17	0.53	Ricker I, 150	± 15	36
18	0.65	Ricker I, 150	± 15	36

Table 2: Overview of the crack density (ρ_{cd}), source signal, dominant frequency (f_{dom}), inclination of the cracks and relation of dominant wave length to crack length used in the experiments displayed in Fig. 2 and Fig. 3.

DISCUSSION AND CONCLUSIONS

Our so far obtained results clearly show the application of the differential schemes to yield much more realistic predictions of effective reflection coefficients for normal incident P-waves than the non-interaction approximation. This agrees with transmission results obtained previously by Saenger et al. Saenger et al. (2004) and Orlowsky et al. Orlowsky et al. (2003) and lets us expect the Differential schemes to be the most reliable also in predicting the offset dependent effective reflection coefficients. So far, we studied the case of a plane P-wave hitting the cracked region at normal incidence. Of great interest is surely the offset dependent behaviour of the reflection coefficient. For this, experiments using a point source and a cautious analysis of the seismograms are necessary, which still are in progress. Fig. 4 shows such synthetic seismograms, which will enable us to determine the amplitude variation vs. offset, i.e. the dependence of the reflection coefficient on the angle of incidence. Note the direct P- and S-wave and the reflected wave field caused by the cracked region. Once more, the rotated staggered grid proves to produce stable and realistic simulations of wave propagation in cracked media.

REFERENCES

Arns, C. H., Knackstedt, M. A., Pinczewski, W. V., and Garboczi, E. J. (2002). Computation of linear elastic properties from microtomographic images: Methodology and agreement between theory and experiment. *Geophysics*, 67:1396–1405.

Bristow, J. (1960). Microcracks and the static and dynamic elastic constants of annealed and heavily cold-worked metals. *British Journal of Applied Physics*, 11:81–85.

Castagna, J. and Backus, M. (1993). Offset-dependent reflectivity - theory and practice of AVO analysis. *Society of Exploration Geophysicists*, page 348pp.

Krüger, O. S., Saenger, E. H., and Shapiro, S. (2002). Simulation of the diffraction by single cracks: an accuracy study. *72th Ann. Internat. Mtg., Soc. Expl. Geophys., Expanded Abstracts*, pages 2007–2010.

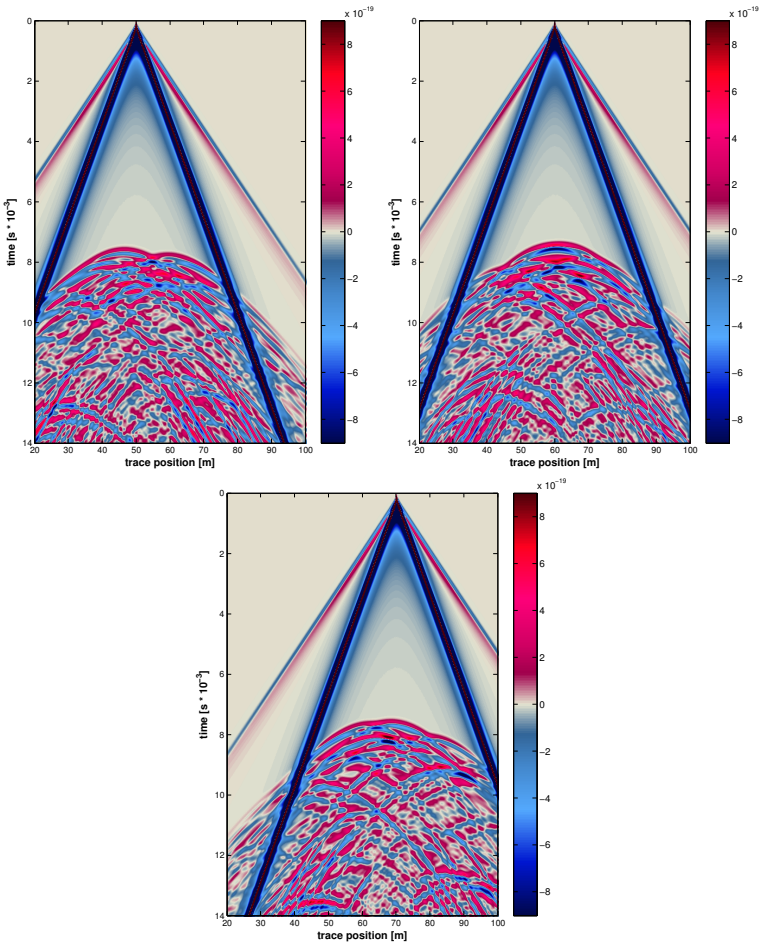

Figure 4: Point source seismograms for the vertical displacement reflected from a cracked region for different shot locations.

Mavko, G., Mukerji, T., and Dvorkin, J. (1998). *The Rock Physics Handbook*. Cambridge University Press, Cambridge.

Orlowsky, B., Saenger, E. H., Guéguen, Y., and Shapiro, S. A. (2003). Effects of parallel crack distributions on effective elastic properties - a numerical study. *International Journal of Fractures*, page in print.

Saenger, E. H., Gold, N., and Shapiro, S. A. (2000). Modeling the propagation of elastic waves using a modified finite-difference grid. *Wave Motion*, 31(1):77–92.

Saenger, E. H., Krüger, O. S., and Shapiro, S. A. (2004). Effective elastic properties of randomly fractured solids: 3D numerical experiments. *Geophys. Prosp.*, 52(3):in print.

Saenger, E. H. and Shapiro, S. A. (2002). Effective velocities in fractured media: A numerical study using the rotated staggered finite-difference grid. *Geophys. Prosp.*, 50(2):183–194.